

SCEC Project 14115

A systematic search for seismic precursors to earthquakes in southern California

PI: Jean-Paul Ampuero (Caltech)

Summary

We have searched for tremor-like precursors to M 2.5-6 earthquakes in southern California. We use a frequency-domain phase coherence technique to examine the 5 minutes before each of 10000 earthquakes. This approach allows us to identify signals coming from the same location as the earthquake, even if those signals come from a source with extended duration. This method successfully detects many previously identified foreshocks, as well as a few foreshocks that are not in the catalog. However, with the methods and data used here, we see no evidence for more emergent seismic signals. This suggests that emergent precursors are rare or small, which is consistent with the infrequent reports of them.

Motivation

Earthquakes are often preceded by foreshocks (e.g., *Felzer et al.*, 2004; *Brodsky*, 2011; *Shearer*, 2012). They are sometimes preceded by aseismic slip or slow deformation (e.g., *Sagiya*, 1998). And in a few cases they have been preceded by tremor-like seismic signals (*Bouchon et al.*, 2011; *Tape et al.*, 2013). The presence or lack of emergent seismic signals is of interest because they could provide information about any aseismic slip leading up to earthquakes. Here we have conducted a systematic search for tremor-like signals prior to earthquakes in southern California.

Summary of the method

Emergent signals are often difficult to detect and locate. In this work, we use a phase coherence technique to analyze them. This method allows us to identify seismic signals coming from the same location as the earthquake, even if those signals are generated by a complex source-time function.

In the phase coherence technique, we examine the Fourier coefficients of two seismograms at each of several stations. These seismograms are hypothesized to result from an earthquake and a precursor that occurred at the same location. In this case, the phases of the Fourier coefficients would result from 2 sets of unknowns: the phases of the two source-time functions, and the phases of the Green's functions for each station. We can eliminate both sets of phases by cross-correlating between sources and then between stations.

This procedure is illustrated with synthetic data in Figure 1. There are four observed signals: 2 from the earthquake and 2 from the synthetic precursor. In the first line, we cross-correlate the earthquake and precursor record at individual stations. This eliminates the Green's functions' phases. We then cross-correlate between stations to eliminate the phases of the source-time functions. Since the synthetic precursor has the same Green's function as the earthquake, the final phase is zero.

One measure of this final phase is the phase coherence. If $\hat{d}_{ej}(\omega)$ and $\hat{d}_{pj}(\omega)$ are the Fourier coefficients of the seismograms observed at station j , the phase coherence between stations 1 and 2 is

$$C = \frac{1}{N} \sum_{\text{frequency}} \text{Re} \left[\frac{\hat{d}_{e1} \hat{d}_{p1}^* \hat{d}_{e2}^* \hat{d}_{p2}}{|\hat{d}_{e1} \hat{d}_{p1}^* \hat{d}_{e2}^* \hat{d}_{p2}|} \right], \quad (1)$$

where there are N frequencies. We incorporate more stations by averaging the phase coherence over station pairs. We also use windowing and multi-taper coherence estimation to improve the robustness of our estimates.

$$\begin{aligned}
\text{Each record: } d(t) &= s(t) * g(t) = \sum_{\omega} \hat{s}(\omega) \hat{g}(\omega) e^{i\omega t} \\
&= \sum_{\omega} S(\omega) e^{i\phi(\omega)} G(\omega) e^{i\theta(\omega)} e^{i\omega t} \\
&= \sum_{\omega} S(\omega) G(\omega) \exp i(\phi(\omega) + \theta(\omega)) e^{i\omega t}
\end{aligned}$$

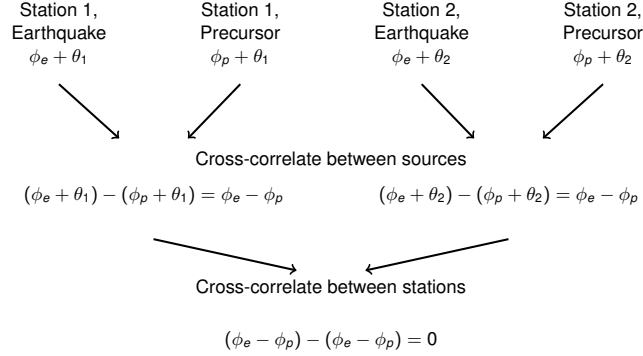


Figure 1: Illustration of the phase coherence approach.

A Search for Precursors

To investigate the occurrence of tremor-like precursors, we examine the 5 minutes before 10000 earthquakes in southern California. We use the earthquake signal as a template, extracting 5 seconds of data starting 0.5 seconds before the catalogued P arrival (*SCEDC*, 2015). We compute the phase coherence between this template and the signal present before the P arrival. For the earlier signals we consider 5-second windows spaced at 2.5 seconds. Most of the seismic data used was collected with the SCSN network (*SCEDC*, 2015), as well as the PBO (Plate Boundary Observatory) and ANZA (UCSD) networks.

One Test Case: A Foreshock

Figure 2c shows an example of the phase coherence before and after a M 3.7 earthquake on the San Jacinto Fault. Away from the earthquake, the coherence is generally small—of order the expected standard deviation (see right hand axis). The phase coherence is high at the time of the earthquake, since the earthquake is coherent with itself. In addition, the coherence is high at the time of a M 2.9 foreshock that occurred 2 km away. Since these two earthquakes are likely to have different source-time functions in part of the 1-10 Hz band, this confirms that the phase coherence technique is able to identify signals with similar path effects but different source-time functions.

To further confirm that our technique should detect tremor-like signals, we convolve the foreshock signal with 5 seconds of white noise. In Figure 2e we have replaced the foreshock signal with this simulation of a more complicated source. As seen in Figure 2f, the phase coherence is still high.

Results of the systematic search

In our search, we use variable amounts of data for each earthquake. To identify the intervals that we are best able to resolve, we use the variance estimates from the multitaper coherence estimation. This provides an uncertainty on the unnormalized phase coherence (the numerator in equation 1), and we use only plot results from intervals where we should resolve a precursory signal that had energy comparable to that expected for a M 2 earthquake.

In addition, we are interested in emergent arrivals, so we discard intervals that are within 10 seconds of catalogued foreshocks.

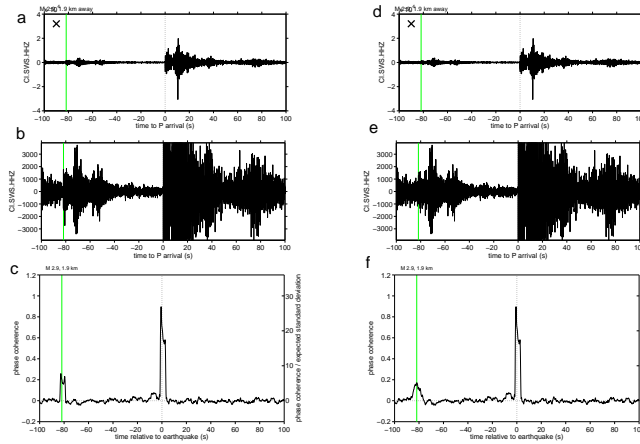


Figure 2: Illustration of the phase coherence method with a M 3.9 earthquake and its M 2.7 foreshock. (a and b) Records of the earthquake and its foreshock at one station. Panel b is an enlarged version of panel a. (c) Phase coherence between the mainshock and windows before and after the earthquake. The phase coherence is high during the foreshock, indicating that the foreshock and mainshock have similar Green's function. (d and e) As in (a and b), but we have extracted the foreshock signal and convolved it with 5 seconds of white noise before replacing it in the seismogram. Phase coherence with the mainshock as a function of time. The coherence is still high at the time of the foreshock, illustrating that the phase coherence can detect nearby signals even if they have complicated source-time functions.

Figure 3 shows a histogram of the remaining phase coherence values, normalized by their expected standard deviation. The phase coherence values obtained 10 seconds before the earthquakes are shown in blue, and those obtained 200 seconds before are in red. The black histogram includes coherence values from all available windows in the 300 seconds before the earthquakes. There is no significant difference between the central parts of the 3 histograms, and the expected standard deviation is a good estimate of the scatter. This implies that most earthquakes are not preceded by emergent seismic signals. If precursors were common, they would be expected more often closer in time to the earthquake, so the 10-second histogram would be shifted to more positive values.

On the other hand, there are a handful of outliers in the low-frequency histograms: intervals with larger phase coherence. There are more positive outliers than negative ones, suggesting that these values result from real signals originating close to the earthquakes. Our search identifies 10 intervals with phase coherence larger than 4 times the standard deviation, and we have examined these visually.

All of the outliers examined so far appear to result from uncatalogued foreshocks. Figure 4 shows one example. The phase coherence (panel c) identifies a coherent signal 5-10 seconds before the M 3.1 earthquake. In the seismogram (panels a and b) we see that this signal has an abrupt onset, suggesting that it is an earthquake. These earthquakes are located to the south of the US networks, which may be why the smaller earthquake is not present in the SCSN catalog.

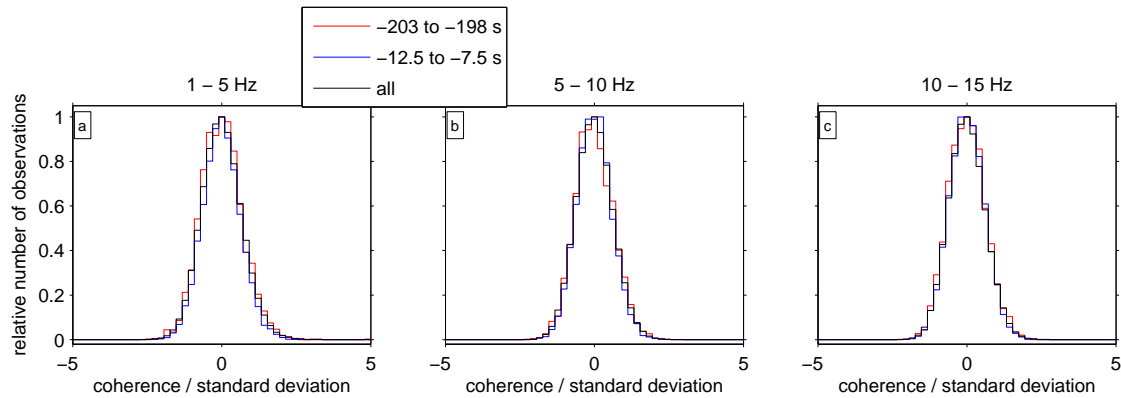


Figure 3: Histograms of the phase coherence values obtained in intervals prior to the earthquake. Intervals with catalogued foreshocks are excluded. The title indicates the frequency range used for the phase coherence calculations.

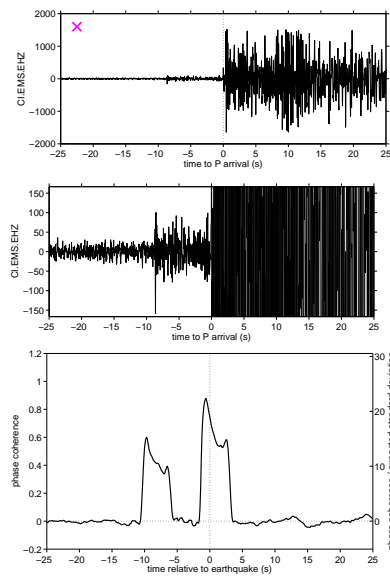


Figure 4: A foreshock detected with our phase coherence search. (a and b) Recordings of a M 3.1 earthquake and a foreshock at one station. The data is the same in both panels. The scale is smaller in panel b. (c) Phase coherence with the M 3.1 as a function of time. The phase coherence is high at the time of the foreshock, suggesting that it is in the same place as the mainshock.

Project Publications

J. C. Hawthorne and J.-P. Ampuero. A search for seismic precursors to earthquakes in southern California. EGU Annual Meeting, April 2015.

J. C. Hawthorne and J.-P. Ampuero. A search for seismic precursors to earthquakes in southern California. SCEC Annual Meeting, September 2014.

References

Bouchon, M., H. Karabulut, M. Aktar, S. Zalaybey, J. Schmittbuhl, and M.-P. Bouin, Extended nucleation of the 1999 Mw 7.6 Izmit earthquake, *Science*, 331(6019), 877–880, doi:10.1126/science.1197341, 2011.

Brodsky, E. E., The spatial density of foreshocks, *Geophysical Research Letters*, 38, L10,305, doi:10.1029/2011GL047253, 2011.

Felzer, K. R., R. E. Abercrombie, and G. Ekström, A common origin for aftershocks, foreshocks, and multiplets, *Bulletin of the Seismological Society of America*, 94(1), 88–98, doi:10.1785/0120030069, 2004.

Sagiya, T., Crustal movements as earthquake precursors —Leveling anomaly before the 1944 Tonankai earthquake revisited, *Bulletin of GSI*, 44, 1998.

SCEDC, Southern California Earthquake Data Center Caltech Dataset, doi:10.7909/C3WD3xH1, 2015.

Shearer, P. M., Self-similar earthquake triggering, Bath's law, and foreshock/aftershock magnitudes: Simulations, theory, and results for southern California, *Journal of Geophysical Research*, 117(B6), B06,310, doi:10.1029/2011JB008957, 2012.

Tape, C., M. West, V. Silwal, and N. Ruppert, Earthquake nucleation and triggering on an optimally oriented fault, *Earth and Planetary Science Letters*, 363, 231–241, doi:10.1016/j.epsl.2012.11.060, 2013.